

Hydrothermal Alteration and Evolution of the Lahendong Geothermal System, North Sulawesi

P. Utami^{1,3}, D.S. Widarto², J.P. Atmojo², Y. Kamah², P.R.L. Browne³, I. W. Warmada¹,
G. Bignall⁴ and I. Chambefort⁴

¹Geothermal Research Centre and Geological Engineering Dept., Faculty of Engineering, GadjahMada University, Indonesia.

²Upstream Technology Centre, PT Pertamina, Jakarta 10110, Indonesia

³The University of Auckland, New Zealand

⁴GNS Science, New Zealand

p.utami@gadjahmada.edu

Keywords: Lahendong, Indonesia, hydrothermal alteration, hydrothermal system evolution

ABSTRACT

The Lahendong geothermal system (North Sulawesi) is the first geothermal system in Eastern Indonesia to be developed for electricity generation. It is also the first geothermal system developed in a tectonically-active arc-arc collision setting. The geothermal system is liquid-dominated and located in steep terrain, with thermal manifestations at about 750 m asl. The field is now penetrated by 28 wells drilled to depths ranging from 1500 to 2500 m, with typical measured temperatures of ~250 °C at about -250 mRSL. The reservoir rocks are mostly andesite and rhyolite that have been radiometrically dated at 2.2 to 0.5 Ma.

Typical hydrothermal (secondary) mineral assemblages at Lahendong at -250 mRSL were formed by near-neutral pH fluids, with occurrences of calc-silicates ± secondary feldspars ± chlorite ± illite ± quartz ± calcite ± hematite. Space-fill mineral paragenesis in drillcore and cuttings recovered from selected wells across the field point to at least five alteration stages (hydrothermal events). Chronologically, the earliest stage is characterized by mono-mineralic veins of chlorite, formed when the system was liquid-dominated. Stage 2 is characterized by calcite and chlorite, and Stage 3 by calcite ± quartz. Stage 4 is marked by calc-silicates ± alkali feldspar, and is inferred to record the peak intensity of hydrothermal activity. Stage 5 is characterized by late-stage calcite, quartz and hematite, with anhydrite conspicuous in the central part of the system, where brecciated veins are common.

Mineralogical evidence has helped resolve the geological evolution of the Lahendong area and highlights thermal and hydrological changes in the system, marked by episodic heating, boiling and cooling, and local fluid mixing in the presently active system (and in inactive/fossil parts of it in the past). Stable isotope analysis of hydrothermal minerals indicates an influx of magmatic fluid at some time into the central part of the system. The Lahendong geothermal system has experienced waxing/waning and relocation of thermal foci, due to sealing and rejuvenation of permeability (e.g. by fault-reactivation) in a long-lived system. These changes may have resulted from a migration of the heat source.

1. INTRODUCTION

Lahendong is a water-dominated geothermal field located in North Sulawesi, Indonesia, approximately 30 km south of Manado, the Capital City of North Sulawesi Province. Two other geothermal fields in this province are Tompaso and Kotamobagu (Figure 1). Lahendong is the first geothermal field in eastern Indonesia to generate electricity and has been producing since 2001. Up to May 2014, 28 wells had been drilled to depths ranging from 1500 – 2500 m, and the field is currently producing 60 MWe. The steam field is managed by PT. Pertamina Geothermal Energy (PGE) and the electricity generation by PT. PLN (State Electricity Enterprise). This paper describes the subsurface hydrothermal alteration of the system, including its mineral parageneses, and reports its spatial and temporal hydrological changes.

2. GEOLOGIC SETTING

2.1 Field overview

Lahendong is part of the Sangihe volcanic arc. It is the only example of an active geothermal system located within an arc-arc collision zone. Here the Sangihe arc over rides the Halmahera arc. The geothermal system is situated about 10 km west of Tondano, a lake which occupies the structure referred to by Newhall and Dzurisin (1998) as the Tondano caldera (20 X 10 km²), of inferred Quaternary age. The active Lokon and Soputan volcanoes are 9 km northwest and 20 km southwest respectively of the system (in Figure 1).

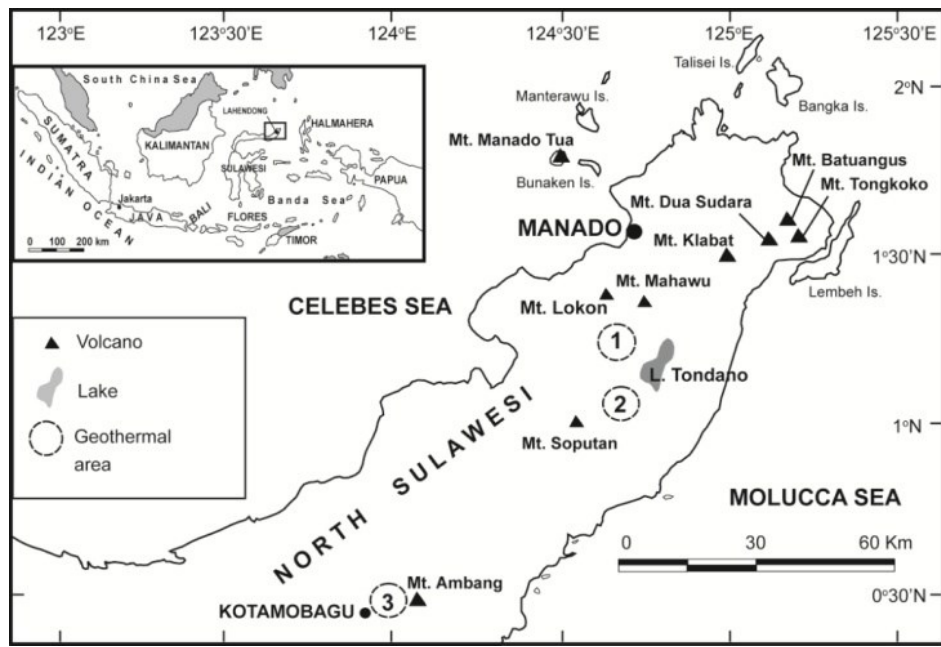


Figure 1: Location of the Lahendong geothermal system (labeled 1, on the map) and the Tompaso (2) and Kotamobagu (3) prospects with respect to major Quaternary volcanoes in North Sulawesi (compiled from Ganda and Sunaryo, 1982; Prijanto et al., 1984; Andan, 1982; Morrice et al., 1983). Inset: Index map shows the position of Lahendong within the Indonesian Archipelago.

The detailed geology of the field was described by Utami (2011) and Pertamina Upstream Technology Center (2013). The system is hosted by volcanic rocks in steep terrain. The rocks cropping out in the field include andesitic lavas and pyroclastics from the eruption centers of Pangolombian, Kasuaratan, Lengkoan, Tampusu and Linau. The system is expressed at the surface by the occurrence of fumaroles and steam-heated active thermal manifestations in Lahendong village and its surrounds at about 750 m above sea level. The thermal manifestations are spatially associated with the Pangolombian horse shoe-shaped structure and Linau crater, as well as faults and joints (Figure 2). The studied wells encountered thick sequences of andesitic – rhyolitic units. From the oldest to the youngest these are: Pre-Tondano andesite, Tondano rhyolite and Post-Tondano andesite. The Pre-Tondano andesite and the Tondano rhyolite units are intruded by diorite dykes (Utami, 2011; Pertamina Upstream Technology Center, 2013).

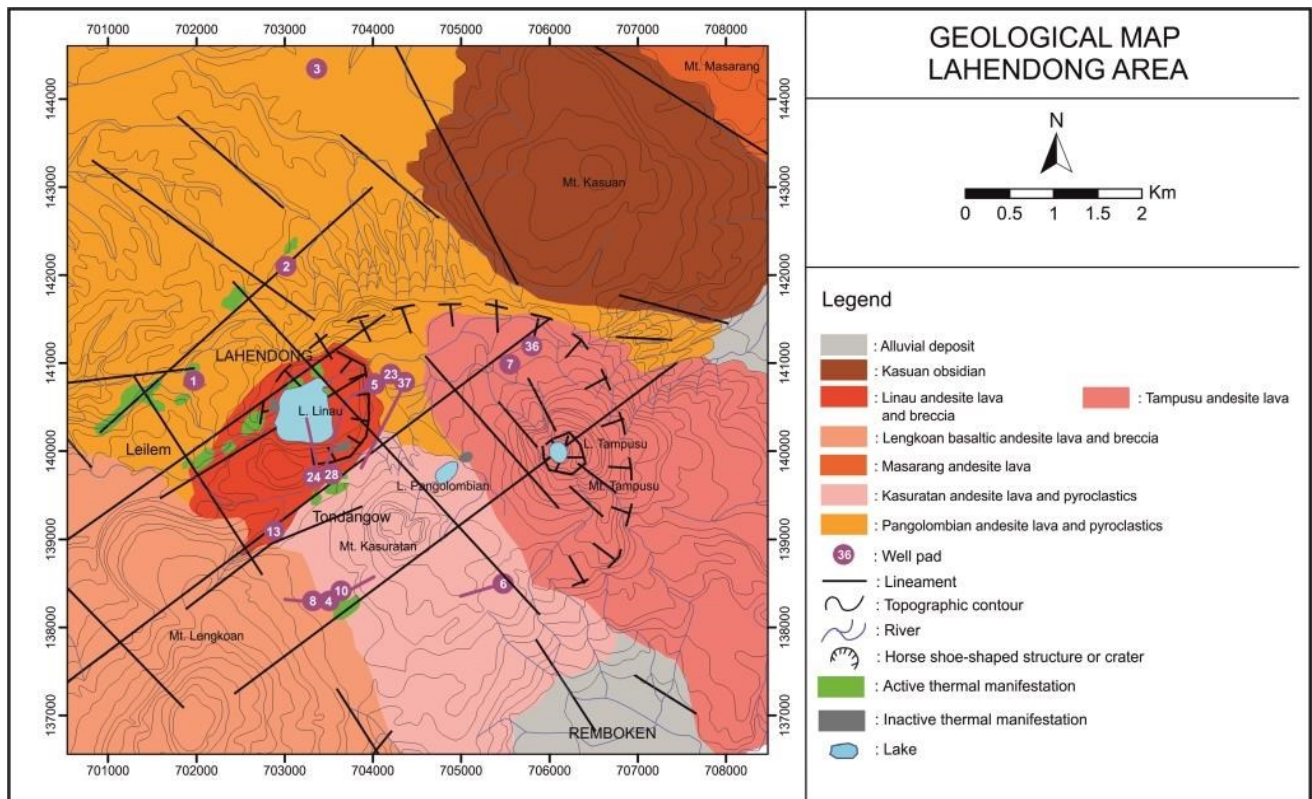


Figure 2: Geological map of the Lahendong Geothermal Field showing the locations of the studied wells (Pertamina Upstream Technology Center, 2013).

2.2 Life of the Lahendong Geothermal System and the Geologic History of the Region

The Sangihe arc is still tectonically and magmatically active (Hamilton, 1988) so the birth and evolution of the Lahendong geothermal system must be viewed in the context of the tectonic and igneous activities of the arc. These are summarized in Figure 3. According to Hamilton (1979), voluminous igneous activity in the Sangihe arc occurred between 14 – 5 Ma. Within that interval (i.e., at about 10 Ma), Sulawesi island (and SE Asia in general) largely attained its present form (Hall, 1997). Based on K/Ar dating of fresh rocks believed to correlate with the altered rocks in the Lahendong system, Utami (2011) estimated that the geothermal system started its activity between 2.2 Ma and 0.5 Ma (Late Pliocene – Middle Pleistocene) ago, i.e., at least 3 Ma after the peak of the voluminous volcanism in the Sangihe arc. If the age estimate of Suari et al (1987) of volcanic activity of Tondano volcano is correct (i.e., Late Miocene or Early Pliocene), then activity of the Lahendong geothermal system began after the Tondano eruptions ceased.

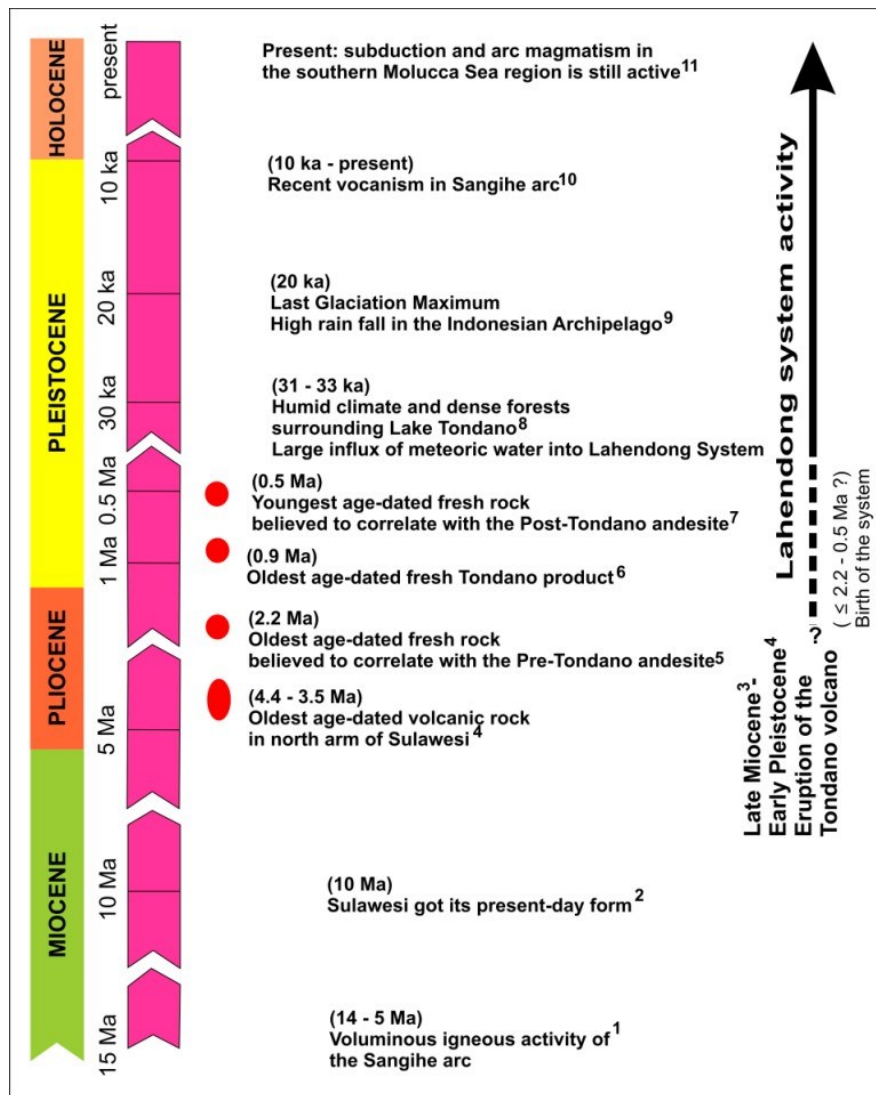


Figure 3: Diagram showing the inferred time of the emergence of the Lahendong geothermal system within the framework of the known geologic history of the north arm of Sulawesi region (Modified from Utami, 2011). References: 1 = Hamilton (1979), 2 = Hall (1997), 3 = Suari et al. (1987), 4 = Morrice et al., (1983), 5 – 7 = PT. Gondwana (1988), 8 = Dam et al., (2001), 9 = Bush and Philander (1999), 10 = Hamilton (1988), Hall (2000), 11 = Macpherson (2003).

3. SAMPLES AND ANALYTICAL METHODS

One hundred cores and 600 bags of cutting samples recovered from 14 of the 28 wells drilled in Lahendong (1500 – 2500 m deep) were examined. The samples were first examined with the aid of a hand lens and a binocular microscope. The selected samples were then thin-sectioned and examined under a petrographic microscope to determine their lithology, the primary and hydrothermal mineralogy, styles of alteration, textures of replacement, as well as the sequence of deposition of vein and other cavity fill minerals.

Bulk rock powders plus clay separates of the selected samples were analyzed by X-ray Diffractometry (XRD). Electron microprobe (EMP) analysis was utilized to support identification of the subsurface primary and hydrothermal minerals. Scanning electron microscopy (SEM) combined with energy dispersive X-ray (EDX) analyses were used to help determine the textural relationships between the minerals in some of the subsurface samples.

Vein minerals were selected for fluid inclusion and stable isotope analyses. Fluid inclusion microthermometry measurements aimed to deduce the temperature and apparent salinity of the fluids circulating in the system at different stages of alteration. Stable isotope analyses were made to figure out the compositions of the altering fluid at the deep, central part of the system.

4. HYDROTHERMAL ALTERATION

4.1 Styles of Alteration

There are 3 alteration styles at Lahendong, namely, leaching/dissolution, replacement, and open space filling. Replacement and dissolution textures record interactions between fluids and the host rocks but the latter involves removal of primary phases without replacing them, to create open spaces. Leaching is obvious in the surface rocks in the steam-heated thermal areas, where phenocrysts, crystal fragments, and even rock fragments were removed. In the subsurface this style of alteration is recognized in the deeper parts of well LHD-3 drilled within the presently inactive thermal area (Utami, 2011), and interestingly, well LHD 24 that was directionally drilled toward Lake Linau (Pertamina Upstream Technology Center, 2013). Replacement involves mass exchanges between individual primary phases and the fluid that moves through intergranular pores. Minerals directly deposited into open spaces (fractures and cavities) record episodic processes that affect the circulating fluids on local scales, such as heating, boiling, cooling, and mixing. The paragenesis of the space-fill minerals was used to infer the sequence of chemical and physical changes that occurred in the circulating fluids.

4.2 Hydrothermal Mineralogy

The hydrothermal minerals in wall rocks in the deeper parts of the system include calc-silicates (zeolites, prehnite, pumpellyite, epidote, clinozoisite, and actinolite), secondary feldspars (albite and adularia), silica minerals (amorphous silica, chalcedony, quartz), clays (smectite, chlorite, illite, and interlayered clays), and calcite. These formed from near neutral pH-alkali chloride waters. Dolomite, Mg-Fe-rich carbonates, anhydrite, and hematite occur locally. The hydrothermal assemblages deposited in open spaces are generally similar to those replacing the primary phases in the wall rock, suggesting that they were formed from fluids of similar compositions. In the deeper parts (-500 to -1300 mRSL) of wells drilled around Lake Linau, anhydrite occurs as both replacement of primary phases and space-fill. This is most likely formed from sulphate-rich waters.

The identity and the distribution of the hydrothermal minerals gives clues about past conditions of the system, most notably former thermal conditions. The past thermal structure of the Lahendong system is deduced from the occurrence of temperature-dependent hydrothermal mineral that replaces the primary minerals field-wide. These include actinolite, epidote, wairakite, and smectite. The common stability temperature ranges of actinolite, epidote, and wairakite, are $\geq 300^{\circ}\text{C}$, 250°C , and 220°C , respectively (e.g., Kristmannsdóttir and Tómasson, 1976; Bird and Helgeson, 1981; Bird, et al., 1984). Smectite is usually stable at temperatures below 150°C (Steiner, 1977). Mordenite and heulandite, which are locally distributed, are stable at temperatures below 200°C (Kristmannsdóttir and Tómasson, 1976). Chlorite is not a reliable temperature indicator since it occurs over a wide range of temperatures, i.e. ~ 140 to $> 300^{\circ}\text{C}$ (e.g., Reyes, 1990; Chatelneau and Nieve, 1985). At Lahendong chlorite is ubiquitous as both a replacement and space-fill mineral. It comprises the early formed veins and was usually the first mineral deposited in multi-mineral veins and other cavities. Textural relations show it was also the first mineral to form through interactions between thermal waters and the primary phases.

4.3 Space-fill Mineral Parageneses

Due to the limited availability of samples, the deduced parageneses are necessarily incomplete records of hydrothermal events at the Lahendong system. Nonetheless, some trends are evident, as follows (Utami, 2011):

1. Simple veins are usually either older or younger than those of complex texture.
2. Chlorite is present field-wide and was commonly the first deposited mineral.
3. Calc-silicates tend to occur in veins with complex textures, which often cut veins with simpler textures, and so may have been formed after them.
4. Brecciated veins (recorded only in some wells) are the youngest.

Space-fill mineral paragenesis suggests that the system has undergone five stages of alteration (Utami, 2011; Pertamina Upstream Technology Center, 2013). The earliest stage is characterised by simple, mono-mineralic veins of chlorite, formed when the system was liquid-dominated. Stage 2 is characterised by calcite and other generations of chlorite, and stage 3 by calcite \pm quartz, which in LHD-4 was joined by other carbonates. Stage 4 is marked by calc-silicates \pm secondary feldspars and is believed to record the peak of hydrothermal activity. Stage 5 is commonly characterised by late calcite, late quartz, hematite, and anhydrite. Anhydrite occurs at the deeper parts of the wells drilled around the Lake Linau, i.e., LHD-1, LHD-5 cluster, LHD-24 and LHD-28, and in LHD-3 that is now a thermally inactive part of the system. Brecciated veins characterised the last stage of alteration in samples recovered from LHD-5 and LHD-1, with chalcedony being the last mineral deposited in LHD-5. Low temperature zeolites, i.e., mordenite and heulandite, developed at shallow depths in LHD-6, and LHD-10 and 13, respectively. Space-fill mineral parageneses of well LHD-5 is shown as an example in Figure 4.

4.4 Stable Isotope Analyses

Seven core samples from LHD-1 and LHD-5 (Chambeuf and Bignall, 2013) and two from LHD-24 and LHD-37 (Pertamina Upstream Technology Center, 2013) were selected for stable isotope analysis. Oxygen, hydrogen, carbon and sulfur isotopes were analysed on hand-picked space-fill quartz, clay, calcite and anhydrite (Table 1). The aim is to identify potential fluid source(s).

The oxygen and hydrogen ranges of isotopic values of the fluid in equilibrium with quartz, calcite and clay samples are shown on Figure 5. Assuming a range of temperature between 250 and 270°C for the precipitation of the quartz, the fluid in equilibrium has $\delta^{18}\text{O}$ varied between 1.36 to 2.21‰ for LHD-1/750 m, 2.55 to 3.4‰ for LHD-5/900-901 m, and -6.18 to -5.33‰ for LHD-1/900-901 m, however, the last sample is likely to be impure quartz (probably calcite contamination). Oxygen isotopes of water in equilibrium with the calcite are calculated using the $\delta^{18}\text{O}_{\text{SMOW}}$ values of the calcite and range between 2.7 and 7‰ at 250°C .

The calculated fluids are isotopically heavier than the meteoric water or the oxygen value of local spring water and are interpreted to contain magmatic-sourced oxygen. This is consistent with the oxygen and hydrogen isotopic values of the fluid in equilibrium with the chlorite (\pm illite) in sample LHD-1/801-802 m (Figure 5). The isotopic value of the fluid was recalculated for 250°C for pure chlorite and also reflects a mixture of magmatic and meteoric oxygen sources. These sources can result from either: 1) a magmatic source where a large component of the fluid is directly exsolved from a degassing magma chamber or; 2) a large “O-shift” due to a low water-rock ratio between ^{18}O -depleted meteoric and/or chloride hot spring water and Lahendong volcanic rocks

with an expected oxygen value $>6\text{\textperthousand}$. The composition of the fluid in equilibrium with chlorite in sample LHD-1/801 m, assuming that a proportion of illite is present in it, is slightly enriched in deuterium compared to the primary magmatic rocks. This also indicates some magmatic oxygen in the system.

Stage Depth (m)	1 ₅	2 ₅	3 ₅	4 ₅	5 ₅
500 - 501	hem	$\begin{matrix} \nearrow \\ \text{cal} \pm \text{qtz} \pm \text{chl} \pm \text{hem} \\ \searrow \end{matrix}$			
650 - 651	chl	(chl \pm cal \pm anh)		tita	
652 - 653	chl chl	$\xrightarrow{\text{cal}}$	$\begin{matrix} \text{qtz} \\ \text{qtz} \end{matrix} \xrightarrow{\text{cal}} \begin{matrix} \text{anh} \\ \text{tita} \end{matrix}$		
750 - 751	chl	$\xrightarrow{\text{cal}}$	$\xrightarrow{\text{chl}}$	$\xrightarrow{\text{cal}}$	$\begin{matrix} \nearrow \\ \text{cha} \end{matrix}$
900 - 902*	chl		(cal \pm anh) \rightarrow (qtz \pm pyr)		
1101 - 1102	chl		qtz	$\xrightarrow{\text{epi}}$	
1102 - 1103	chl	(ill $\xrightarrow{\text{qtz}}$)		$\begin{matrix} \text{czo} \\ \text{epi} \\ \text{tita} \end{matrix}$	$\begin{matrix} \nearrow \\ \text{qtz} \end{matrix}$
1301 - 1302			chl, ill, cal, qtz, epi, tita, adu, pyr		$\begin{matrix} \nearrow \\ \text{micr. qtz} \end{matrix}$
1331 - 1332	chl		(chl \pm qtz)		
1404 - 1405	chl	(cal - qtz) (micr. qtz \pm pyr \pm epi)		$\xrightarrow{\text{cal}}$	

Figure 4: Summary of space-fill mineral paragenesis in LHD-5. Abbreviations: chl = chlorite; ill = illite; cal = calcite; qtz = quartz; cha = chalcedony; micr. qtz = microcrystalline quartz; tita = titanite; epi = epidote; czo = clinozoisite; adu = adularia; pyr = pyrite; arrow = mirror-type vein; \pm = segmental-type vein; ; wiggled line = fracturing event; wiggled line with triangles = vein brecciation event.

Table 1: Carbon, oxygen and hydrogen stable isotope values for selected Lahendong samples.

Sample	Mineral	$\delta^{13}\text{C}$ Value	$\delta^{18}\text{O}$ Value	δD Value	$\delta^{34}\text{S}$ Value
LHD-1/750 m	quartz		10.32		
LHD-1/801-802 m	calcite	-1.49	-15.76		
LHD-1/801-802 m	clay#		6.1	-74.9	
LHD-1/900-901 m	calcite	-3.33	-18.87		
LHD-1/900-901 m	quartz*		2.78		
LHD-1/1452-1453 m	calcite	-0.83	-20.30		
LHD-5/900-901 m	quartz		11.51		
LHD-24/2173 m	anhydrite		14.40		3.00
LHD-37/2228 m	anhydrite		3.20		5.90

*Mainly consists of chlorite with rare illite.

* Sample is likely not pure quartz.

The isotopic compositions of oxygen and sulfur shows that the rocks from deeper parts of wells LHD-24 and LHD-37 got a pulse of magmatically-derived fluids at some time (Figure 6). Anhydrite from LHD-24 has isotopic values similar to the hypogene anhydrite deposited in high sulphidation epithermal environments such as those that occurred at Ladolam, Papua New Guinea (Gemmell et al., 2004), Butte, USA (Field et al., 2005), and Chelopech, Bulgaria (Chambeffort, 2005). Anhydrite from the deeper well LHD-37 probably deposited from magmatic SO_2 gas, or oxidised H_2S magmatic gas. This magmatic-hydrothermal environment was similar to a magmatic ore depositing environment.

The carbon isotope value of the fluid was recalculated for 250°C assuming that the calcite was in equilibrium with CO_2 . $\delta^{13}\text{C}_{\text{CO}_2}$ contents range between -2.03 and $0.47\text{\textperthousand}$. Mantle (e.g. magmatic) carbon has an isotopic value varying between -8 and $-4\text{\textperthousand}$, oceanic carbon has a value of $\sim 0\text{\textperthousand}$. Chambeffort and Bignall (2013) suggested that a portion of the carbon assimilated by calcite originated from nearby marine sediments. This interpretation is consistent with the occurrence of fossil-rich tuffaceous siltstone intercalations that occur in deeper parts of the system as parts of the Pre-Tondano unit (Utami, 2011).

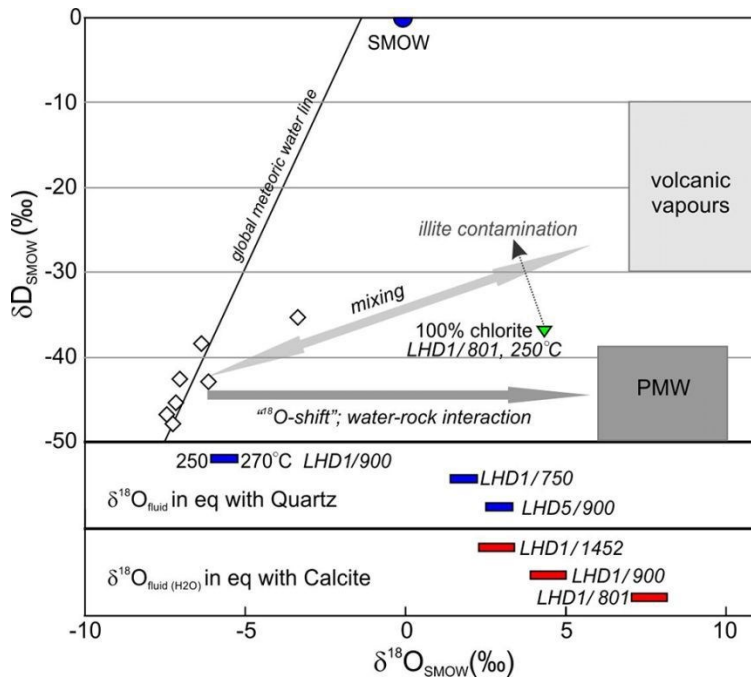


Figure 5: Plot of δD and $\delta^{18}\text{O}$ isotopic values of the calculated fluids in equilibrium with Lahendongclay and $\delta^{18}\text{O}$ values of water in equilibrium with quartz and calcite (blue and red bars, respectively, calculated for between 250 and 270°C). The temperatures are estimated from fluid inclusions and well temperatures from Utami (2011). White diamonds are Lahendong spring waters from Utami (2011). Volcanic vapours field is from Giggelnbach (1992), PMW (primary magmatic waters) from Taylor (1979). Diagram from Chambefort and Bignall (2013).

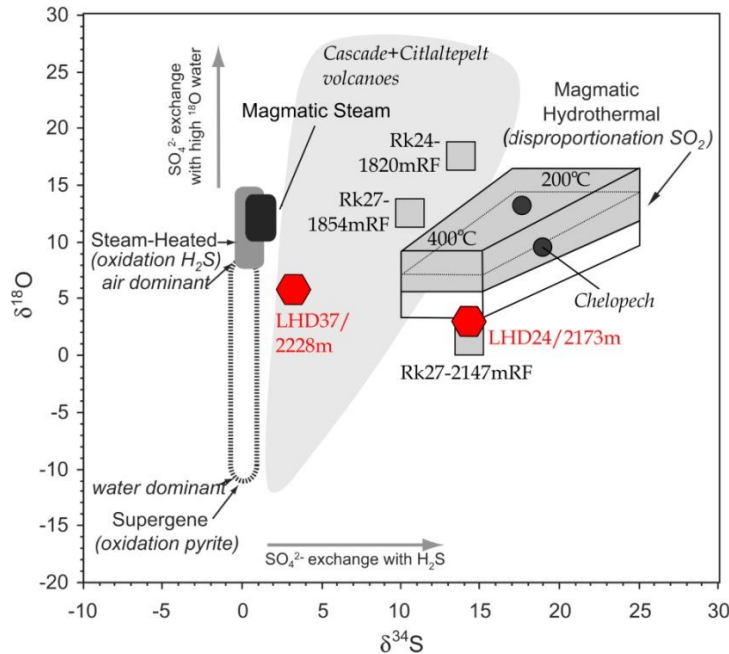


Figure 6: $\delta^{34}\text{S}_{\text{SO}_4}$ versus $\delta^{18}\text{O}_{\text{SO}_4}$ plot of late stage anhydrite from Lahendong on a diagram taken from Chambefort et al (2011) showing the isotopic compositions of anhydrite samples from Rotokawa Geothermal Field (New Zealand) and Chelopech epithermal deposit (Bulgaria), and anhydrite from hydrothermal-magmatic, magmatic-steam, steam-heated and supergene environments.

5. EVOLUTION OF THE LAHENDONG GEOTHERMAL SYSTEM

5.1 The Initiation of the System

The earliest hydrothermal activity started at Kasuratan, i.e., at the area now penetrated by LHD-13. The heat source was likely magmatic, although this was not reached by LHD-13 and later wells (LHD-16 and 18) drilled from the same pad. The activity was marked by the field-wide formation of chlorite from 800 mRSL down to -400 mRSL both replacing primary minerals (in Figure 7A) and occurring in open spaces.

The altering fluid was likely a near neutral pH, alkali chloride water, and the temperature was above 100°C. The main recharge fluid was meteoric water, as suggested by Prijanto et al (1984). This conclusion is supported by the results of paleoclimatological studies by others. For example, Dam et al (2001) indicated that high rainfall in Tondano and its surround occurred in 33 – 31 ka. Simulation of climate conditions by Bush and Philander (1999) showed that there was higher rainfall in the Indonesian Archipelago during the Last Glaciation Maximum (LGM), i.e., ~ 20 ka. This likely provided large groundwater influx into the Lahendong system (in Figure 3).

As the hydrothermal system developed, calcite and quartz were formed followed by calc-silicates such as incipient epidote, titanite and actinolite. A paleotemperature of 300°C, or perhaps higher, was shallowest at LHD-13 (i.e. at -373 mRSL) as recorded by the shallowest occurrence of replacement actinolite. As Utami (2011) deduced that the early system was hotter than now, the shallowest occurrence of replacement actinolite in LHD-13 (indicating a paleotemperature $\geq 300^{\circ}\text{C}$) support the interpretation of the occurrence of the earliest known thermal focus hereafter named the Early Kasuratan thermal focus (Figure 7B). Thermal activity at this focus declined after a boiling event followed by cooling. This is marked by deposition of later calcite, quartz, hematite, and low temperature zeolites (mordenite and heulandite) in the southern sector (Utami, 2011).

5.2 The Shift and the Revival of the Focus of Thermal Activity

The thermal activity then shifted to Pangolombian, i.e., the area now penetrated by LHD-7. This is indicated by the shallowest occurrence of epidote, which indicates a paleo temperature of 250 °C, centered on Pangolombian village (LHD-7) on the eastern margin of the Pangolombian structure (Figure 7C). This thermal focus is named the Early Pangolombian thermal focus. The most likely explanation for the cause of this shift was the self sealing of the permeability at Kasuratan and the development of vertical permeability at Pangolombian that helped channel thermal fluid flow there. Relict steam-heated thermal manifestations occur in Pangolombian village (Pertamina Upstream Technology Center, 2013). The timing of this shift in activity is unknown.

The peak activity of the Early Pangolombian thermal focus was marked by the formation of calc-silicates, including wairakite and epidote. Replacement epidote, indicating temperatures above 250 °C, was shallowest in LHD-7 i.e., 347 mRSL, but deeper in other wells and absent from LHD-3. The Lahendong - Linau area, i.e., that penetrated by LHD-1 and cluster LHD-5 started to heat up but the most northern part of the system (represented by LHD-3) started to cool. The southern sectors (LHD-13 and cluster LHD-4) continued cooling, except the area now penetrated by LHD-6 heated.

The thermal focus again shifted, this time to the Lahendong – Linau area. This is interpreted from the shallowest appearance of wairakite and the deepest appearance of smectite which represent paleo temperatures of 220 and $\leq 150^{\circ}\text{C}$, respectively, that occur in the Lahendong – Linau area now penetrated by LHD-1, LHD-5 cluster and LHD-24 and 28 (Figure 7D). This new focus is henceforth named the Lahendong-Linau thermal focus. This shift is speculated to be due to an eruption, centred at the area presently occupied by Lake Linau, which generated vertical permeability. If so, the shift might have taken place less than 0.5 Ma, as deduced from the age of the rocks produced by the Linau eruption center. The sudden pressure release caused an influx of silica-saturated fluid into the open spaces that deposited quartz as it cooled. This event produced the botryoidal chalcedony that was the last mineral deposited in LHD-5 cluster (Utami, 2011; Pertamina Upstream Technology Center, 2013). The position of the Lahendong – Linau thermal focus has not changed since then. The deepest occurrence of smectite (Figure 7E) suggests the position of the top of high-temperature reservoir at the time this mineral formed. The results of the stable isotope analyses of the minerals formed at late stages in the deeper parts of Lahendong – Linau area (LHD-1, 5, 24 and 37) suggest there was an influx of magmatic fluid at some time into this central part of the system.

The present-day thermal foci are deduced from the measured well temperatures (as represented by the isothermal map at -750 mRSL, in Figure 7F). At present there are two main thermal foci, namely the Lahendong – Linau and the Late Kasuratan, and a minor thermal focus at Pangolombian that is recognized in the deeper parts of LHD-36. At the surface, the Lahendong – Linau and the Late Kasuratan thermal foci are expressed by steam-heated and fumarolic thermal manifestations, but the minor Late Pangolombian thermal focus has not developed any surface expression. The present-day thermal foci are speculated to be due to emplacement of new heat source(s) not penetrated by the existing wells, and/or rejuvenation of permeability.

Despite the absence of age dates, the occurrence and distribution of hydrothermal minerals provide clues about the initiation of the system and the relative timing of its thermal and hydrological changes, as summarized in Figures 8. For convenience, the area penetrated by wells LHD-13, those in LHD-4 cluster, and LHD-6 are referred to as the southern sector (Figure 8A), and the others (i.e., those penetrated by LHD 1, 2, 3, 7, and the LHD-5 cluster) the northern sector (Figure 8B).

6. CONCLUSIONS

Geothermal activity at Lahendong started after the peak of the voluminous volcanism in the Sangihe arc, i.e., between 2.2 Ma and 0.5 Ma ago. The recharge fluid is mainly meteoric water; this has been abundant since ~31 to 30 ka ago. Hydrothermal processes in the deeper parts of the system produced different proportions of silica, secondary feldspars, calc-silicates, clays (including chlorites), carbonates, oxides, sulphides and sulphates in the wall rocks and veins.

Our study shows that it is possible to unravel the history of a hydrothermal system based on its hydrothermal alteration mineralogy. The Lahendong geothermal system has undergone natural changes, most notably shifts in its thermal foci, and slight changes in the composition of the altering fluid. Rocks retrieved from fourteen out of a total 28 deep wells (1500 – 2500 m) show that the system was dynamic and different parts of it have had different hydrothermal histories. At present the system has two major thermal foci, namely the Lahendong – Linau and the Late Kasuratan (both are expressed by active steam-heated manifestations), and the minor Late Pangolombian thermal focus, that has not developed a surface geothermal expression.

The deep, central part of the system (beneath the Linau area) may have experienced pulse(s) of magmatic fluids at some past time as evident from its mineralogy and stable isotope compositions. This finding, combined with the composition of the present-day fluid in this part of the field, needs to be taken into account when making the field development strategy. The behavior of a geothermal

system is better understood if both past and present conditions are known. Reconstructing the way a geothermal system changes through time – starting with observing the rocks – is therefore of similar importance to modelling present-day and future conditions by means of reservoir simulation softwares.

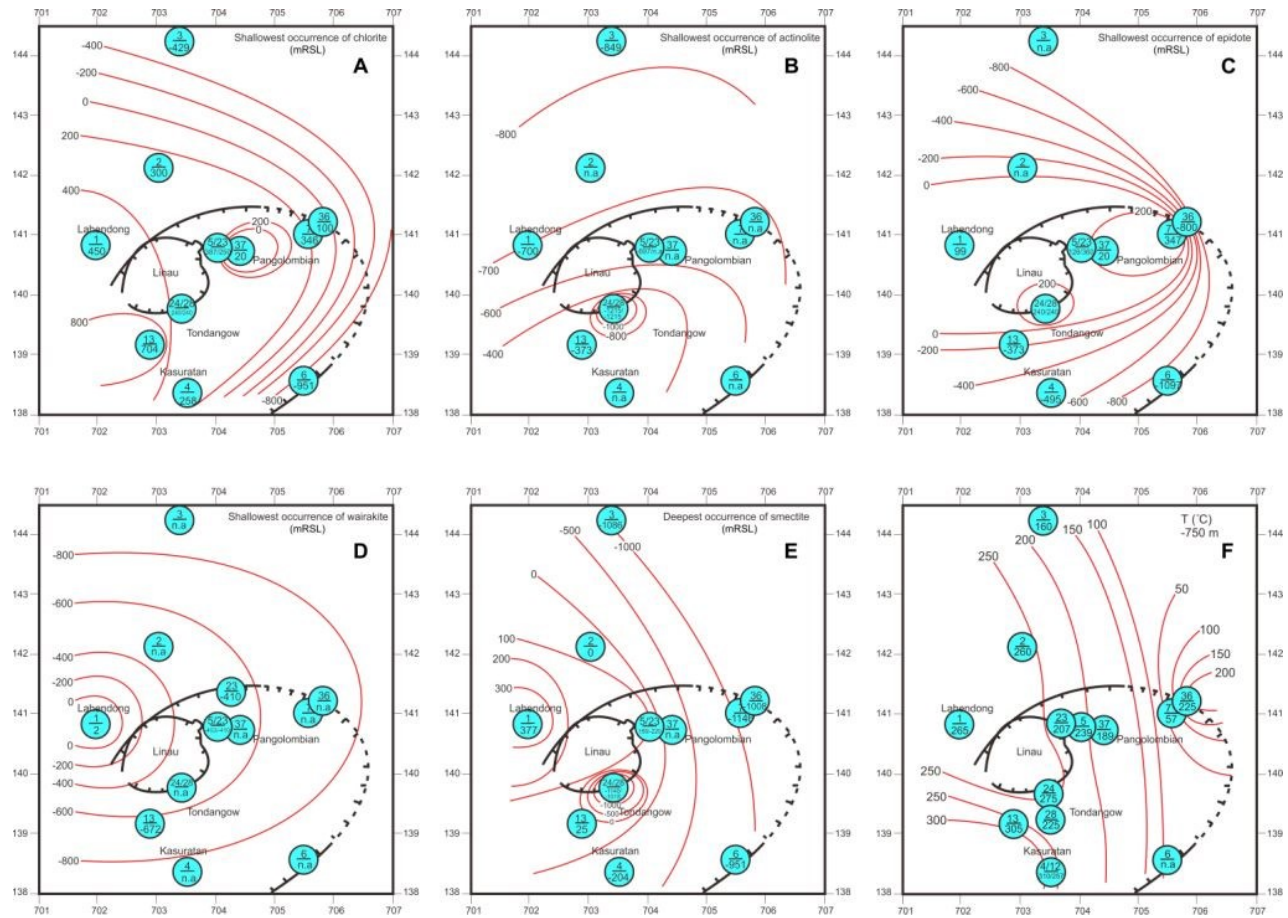


Figure 7: Maps of the shallowest occurrence of chlorite (A), actinolite (B), epidote (C), wairakite (D), deepest occurrence of smectite (E), and the present-day isotherms at -750 mRSL (F), representing the past and present-day thermal structures of the Lahendong geothermal system (compiled from Pertamina Upstream Technology Center, 2013). Blue circles indicate both well number and the shallowest/deepest occurrence of mineral (A-E) in mRSL and the temperature in °C (F).

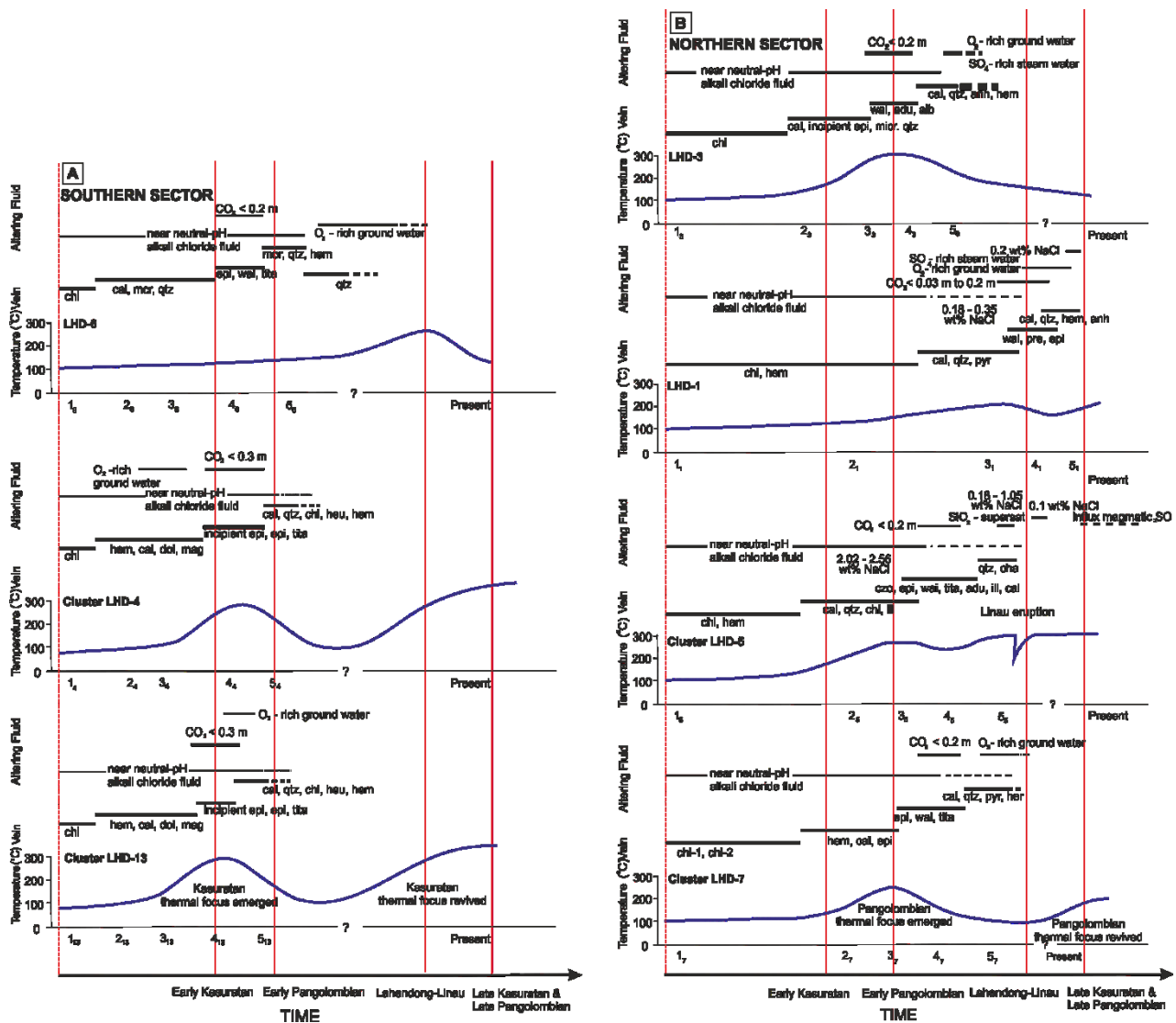


Figure 8: Diagrams summarising the thermal evolution, vein mineralogy and changes in fluid compositions in the southern (A) and northern (B) sectors of the Lahendong geothermal system. Time axis is qualitative. The temperature versus time curves are constructed based on the stability of the calc-silicate minerals occurring as replacements with the time span estimated from the stages of vein mineralisation (numbers with subscripts). Fluid inclusion homogenisation temperatures included where available. Broken red lines indicate the timing of the emergence of the thermal foci.

7. ACKNOWLEDGEMENTS

Parts of this work involving wells LHD-1, 3, 4, 5, 6, 7, 8, 10, 12 and 13 was conducted at The University of Auckland during the PhD study by the first author funded by an NZAID Open Scholarship (2004 – 2008). The Indonesian Ministry of Education and Culture is thanked for funding of the stable isotope analyses of selected hydrothermal minerals at GNS Science, New Zealand in 2013. Analyses of rock samples from LHD-23, 24, 28, 36 and 37 were made under the collaboration between Faculty of Engineering UGM and Pertamina Upstream Technology Centre in 2013. The authors thank the Managements of PT. PGE and Upstream Technology Centre of PT. Pertamina Ltd. for permission to publish this paper. Ms. Kinanti Hapsari of Geothermal Research Centre Faculty of Engineering UGM is thanked for assisting with the drafting of the graphs and formatting the manuscript.

8. REFERENCES

Andan, A.: Scientific studies of the Kotamobagu geothermal prospect, North Sulawesi, Indonesia, Project for Diploma in Energy Technology, Geothermal Institute, The University of Auckland, (1982).

Bird, D.K., and Helgeson, H.: Chemical interactions of aqueous solutions with epidote - feldspar mineral assemblages in geologic systems. II: Equilibrium constraints in metamorphic/geothermal processes, *American Journal of Science*, **281**, (1981), 576 - 614.

Bird, D.K., Schiffman, P., Elders, W.A., and Williams, A.E.: Calc-silicate mineralisation in active geothermal systems, *Economic Geology*, **79**, (1984), 671 - 695.

Bush, A.B.G., and Philander, S.G.H.: The climate of the Last Glacial Maximum: Results from a coupled atmosphere – ocean general circulation model, *Journal of Geophysical Research*, **104**, (1999), 24509 - 24525.

Cathelineau, M., and Nieva, D.: A chlorite solid solution geothermometer; the Los Azufres (Mexico) geothermal system: Contributions to Mineralogy and Petrology. v. 91; 3, (1985), 235-244.

Chambefort, I.: The Cu-Au Chelopech Deposit, Panagyurishte District, Bulgaria: Volcanic Setting, Hydrothermal Evolution and Tectonic Overprint of Late Cretaceous High-Sulphidation Epithermal Deposit. PhD thesis, University of Geneva, Terre et Environnement, 52,(2005), 173 p.

Chambefort, I., McCoy-West, A., Ramirez, L.E., Rae, A.J., Bignall, G.: Evidence for magmatic fluid pulses into the Rotokawa geothermal system, *New Zealand Geothermal Workshop 2011 Proceedings*, 21-23 November 2011, Auckland, New Zealand, (2011).

Chambefort, I., and Bignall, G.: Preliminary stable isotope study on the Lahendong geothermal system, Indonesia, GNS Report 2013/14, May 2013, (2013).

Dam, R.A.C., Fluin, J., Suparan, P., and van der Kaars, S.: Paleoenvironmental developments in the Lake Tondano area (N. Sulawesi, Indonesia) since 33,000 yr B.P.: Palaeogeography, Palaeoclimatology, Paleoecology, **171**, (2001), 147 - 183.

Field, C.W., Zhang, L., Dilles, D.H., Rye, R.O., Reed, M.H.: Sulfur and oxygen isotopic record in sulfate and sulfide of early, deep, pre-main stage porphyry Cu-Mo and late stage base-metal mineral deposits, Butte district, Montana. Chemical Geology 215, (2005), 61-93.

Gammell, J.B., Sharpe, R., Jonasson, I.R., Herzog, P.M.: Sulfur isotope evidence for magmatic contributions to submarine and subaerial gold mineralization: Conical Seamount and the Ladolam Gold deposit, Papua New Guinea, *Economic Geology*, **99**, (2004), 1711-1725.

Ganda, S., and Sunaryo, D.: A Preliminary Report on Geology of the Minahasa Area, North Sulawesi (in Indonesian), Internal Report, Jakarta, Pertamina Geothermal Division, (1982), 1 - 40.

Gondwana, P.T.: Magmatic Evolution and Geochronology of the Volcanic Activities at the Lahendong Area, North Sulawesi (in Indonesian). Report for PERTAMINA, (1988).

Hall, R.: Cenozoic tectonics of SE Asia and Australasia, Petroleum System of SE Asia and Australasia, Jakarta, (1997), 47 – 62.

Hall, R.: Neogene history of collision in the the Halmahera region, Indonesia, *Proceedings, 27th Indonesian Petroleum Association Annual Convention*, Jakarta, (2000), 487 - 493.

Hamilton, W.B.: Tectonics of the Indonesian Region (Geological Survey Professional Paper 1078), Washington, United States Government Printing Office, (1979), 345 p.

Kristmannsdóttir, H., and Tómasson, J.: Nesjavellir - hydrothermal alteration in a high temperature area, in Čadek, J., and Pačes, T., eds., *International Symposium on Water-Rock Interaction 1974*, Czechoslovakia, The Geological Survey of Prague, (1976), 170 – 177.

Hamilton, W.B.: Plate tectonics and island arc, *Geological Society of America Bulletin*, **100**, (1988), 1503 - 1527.

Macpherson, C.G., Forde, E.J., Hall, R., and Thirlwall, F.: Geochemical evolution of magmatism in arc-arc collision: the Halmahera and Sangihe arcs, eastern Indonesia, in Larter, R.D., and Leat, P.T., eds., *Intra-Oceanic Subduction Systems: Tectonic and Magmatic Processes*, Geological Society of London, (2003), 207 - 220.

Morrice, M.G., Jezek, P.A., Gill, J.B., Whitford, D.J., and Monoarfa, M.: 1983, An introduction to the Sangihe arc volcanism accompanying arc-arc collision in the Molucca Sea, Indonesia, *Journal of Volcanology and Geothermal Research.*, **19**, (1983), 135 - 165.

Newhall, C.G., and Dzurisin, D.: 1988, Historical Unrest at Large Calderas of the World, *U.S. Geological Survey Bulletin*, **1855**, (1988), 345-351.

Pertamina Upstream Technology Center.: The study of the Evolution of Thermal Structures and the Possibility of Magmatic Fluids Inputs into The Lahendong Geothermal System (in Bahasa Indonesia), Project Report for PertaminaUpsteam Technology Center, Faculty of Engineering UGM. Contract No. 47/D30140/2013-SO, (2013).

Prijanto, Fauzi, A., Lubis, L.I., and Suwana, A., 1984, Geochemistry of the Minahasa Geothermal Prospect, North Sulawesi, *Proceedings, 13th Indonesian Petroleum Association Convention*: Jakarta, (1984), 473 - 485.

Reyes, A.G., 1990, Petrology of the Philippine geothermal systems and the application of alteration mineralogy to their assessment, *Journal of Volcanology and Geothermal Research*, **43**, (1990), 279 - 309.

Steiner, A.: The Wairakei geothermal area, North Island, New Zealand: its subsurface geology and hydrothermal rock alteration, Wellington, Dept. of Scientific and Industrial Research, (1977), 1 - 135.

Suari, S., Tandirerung, S.A., Buntaran, T., and Robert, D.: Assessment of the Lahendong Geothermal Field, North Sulawesi, Indonesia, *Proceedings, 16th Indonesian Petroleum Association*, (1987).

Taylor, H.P.Jr.: Oxygen and hydrogen isotope relationships in hydrothermal minerals deposit: In geochemistry of hydrothermal ore deposits, 2nd ed., Barnes, H.J. (ed), New York, John Wiley, (1979), 236-277.

Utami, P.: Hydrothermal Alteration and the Evolution of the Lahendong Geothermal System, North Sulawesi, Indonesia. Ph.D. Thesis. The University of Auckland, (2011), 449 p.